

Electronic Supplementary Information

Synthesis and characterization of novel electrochromic poly(amide-imide)s with *N,N'*-di(4-methoxyphenyl)-*N,N'*-diphenyl-*p*-phenylenediamine units

Sheng-Huei Hsiao,^{*a} Chia-Yin Teng,^a Yu-Ruei Kung,^b

^aDepartment of Chemical Engineering and Biotechnology, National Taipei University of Technology, Taipei 10608, Taiwan. Correspondence to: S.-H. Hsiao (E-mail: shhsiao@ntut.edu.tw)

^bDiv. of Organic Opto-electronic Materials and Applications, Material and Chemical Laboratories, Industrial Technology Research Institute, Hsinchu 31040, Taiwan.

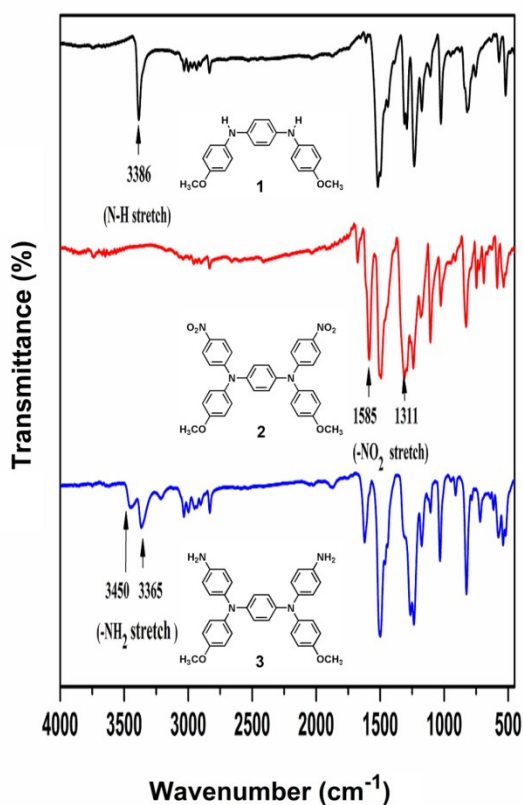


Fig. S1 IR spectra of synthesized compounds 1–3.

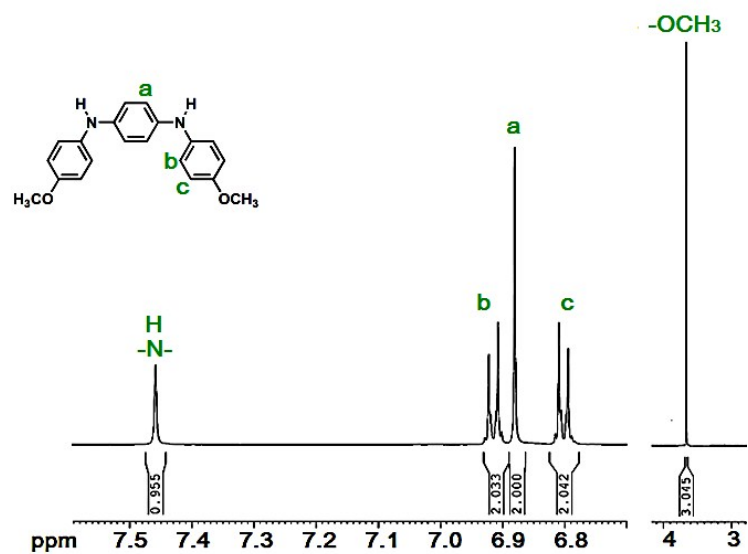


Fig. S2 The ¹H-NMR spectrum of compound 1 in DMSO-*d*₆.

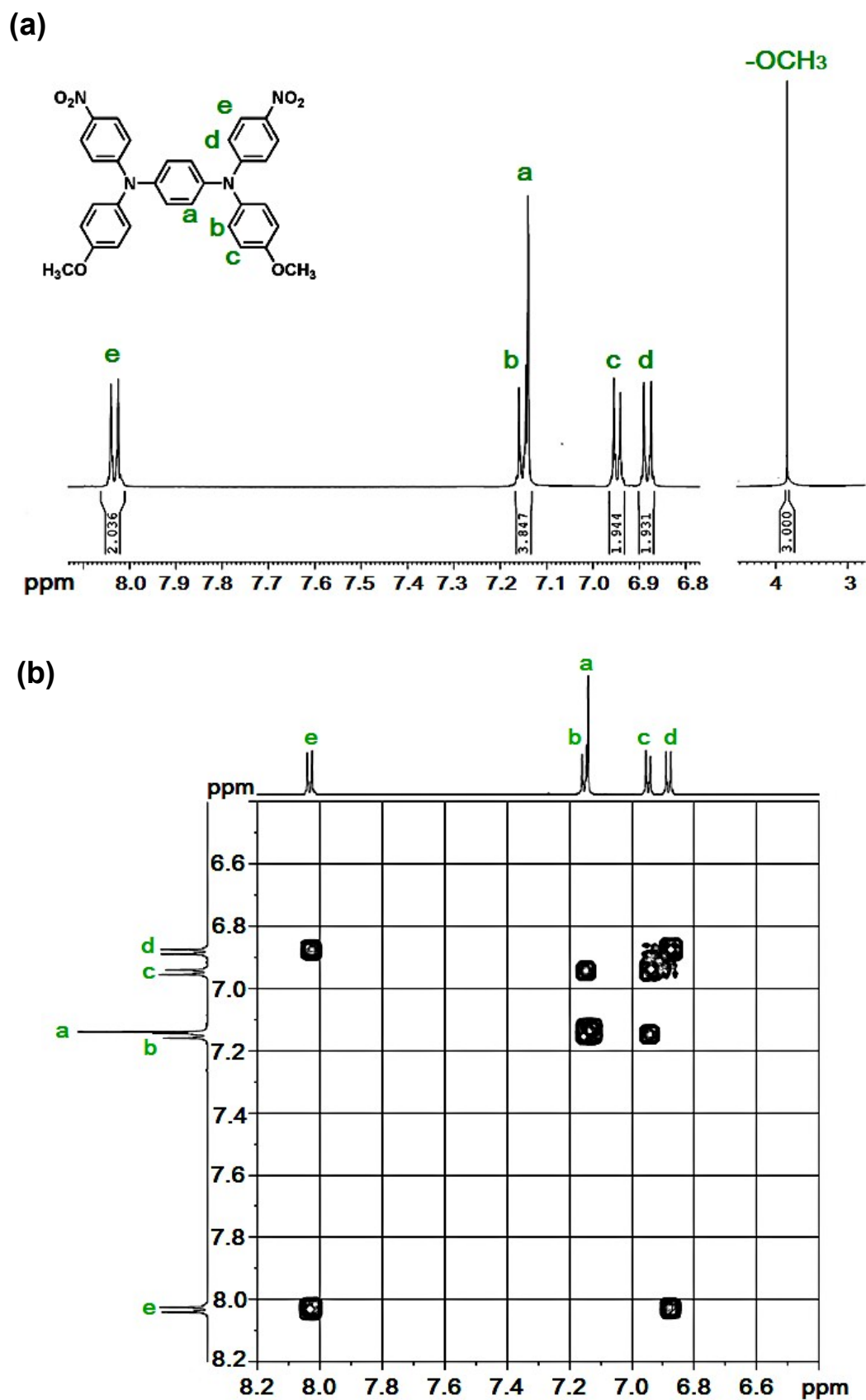


Fig. S3 (a) ^1H and (b) H-H COSY NMR spectra of dinitro compound **2** in CDCl₃.

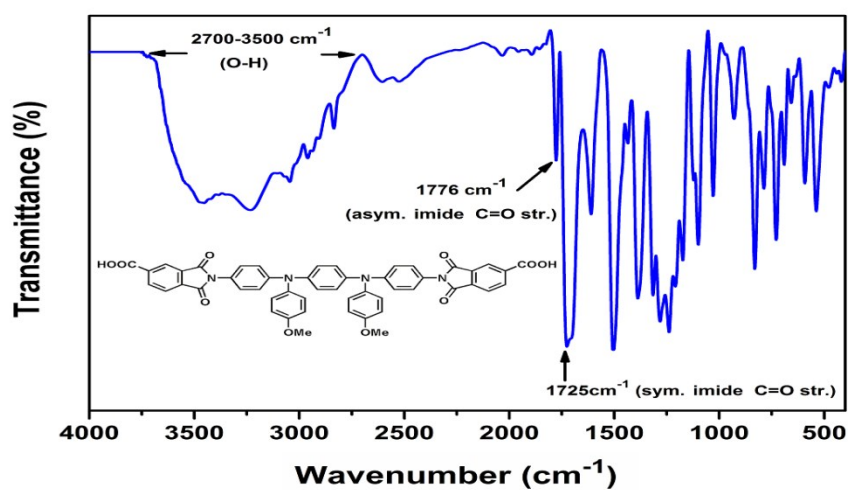


Fig. S4 The IR spectrum of diimide-diacid monomer 4.

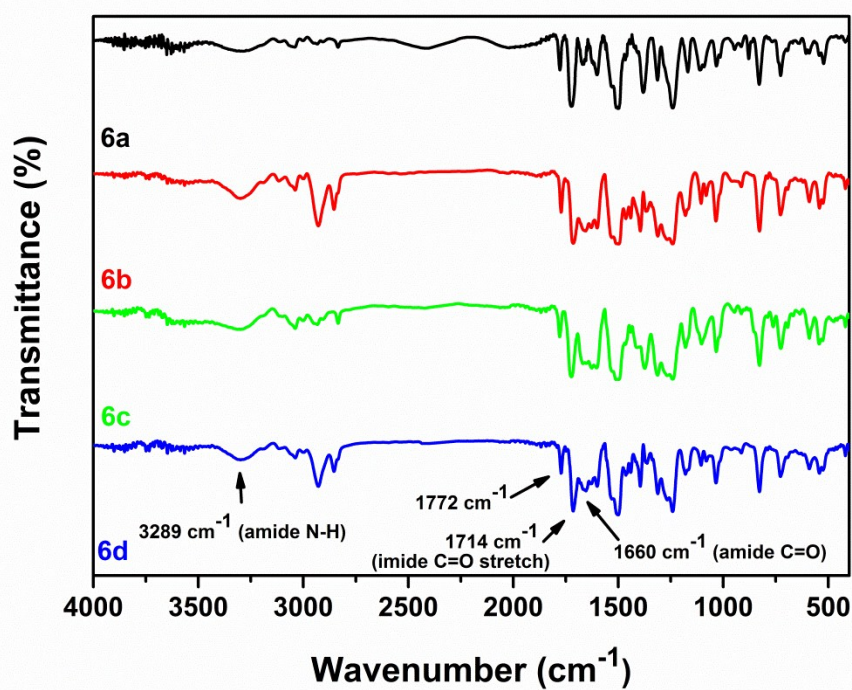


Fig. S5 IR spectra of PAIs 6a-6d.

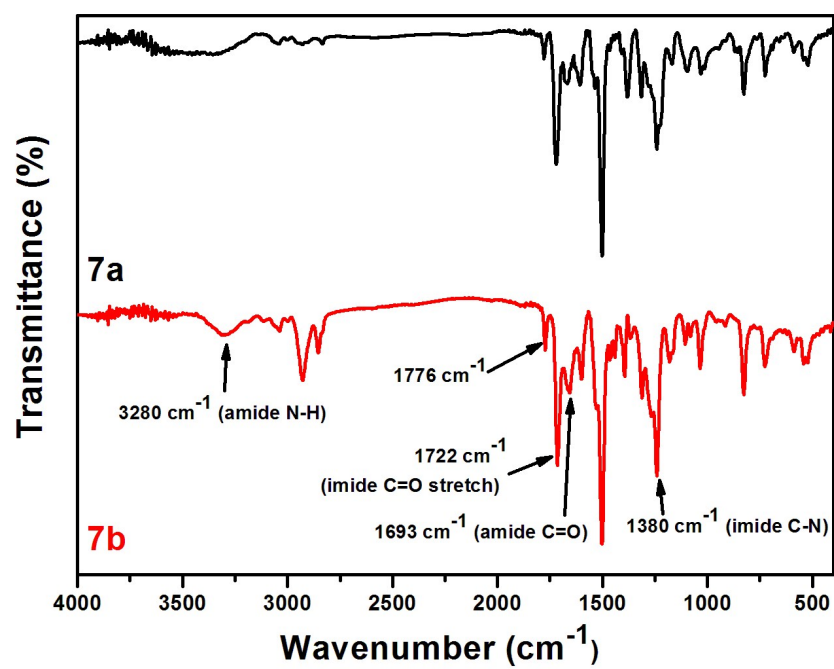
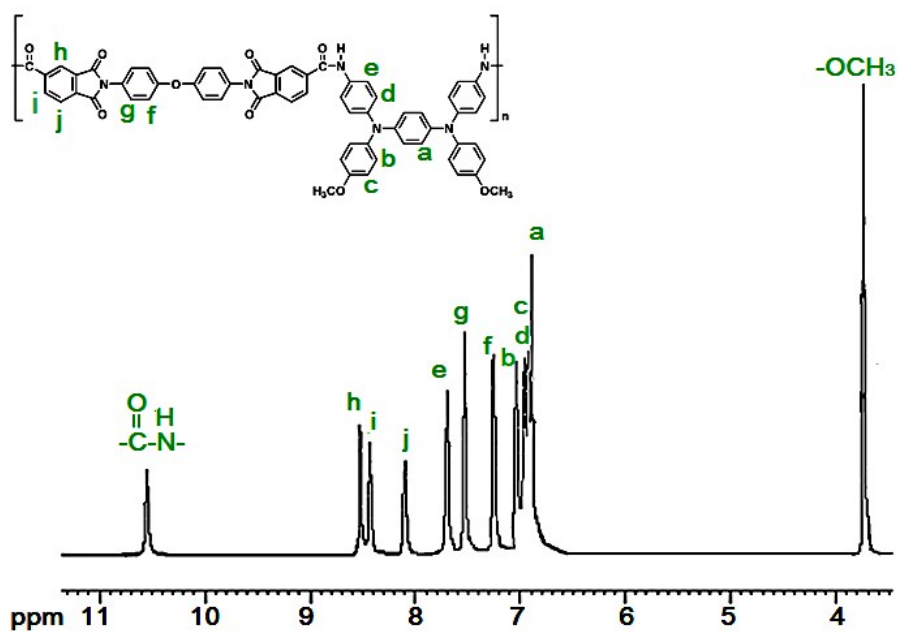


Fig. S6 IR spectra of PAIs **7a** and **7b**.

(a)



(b)

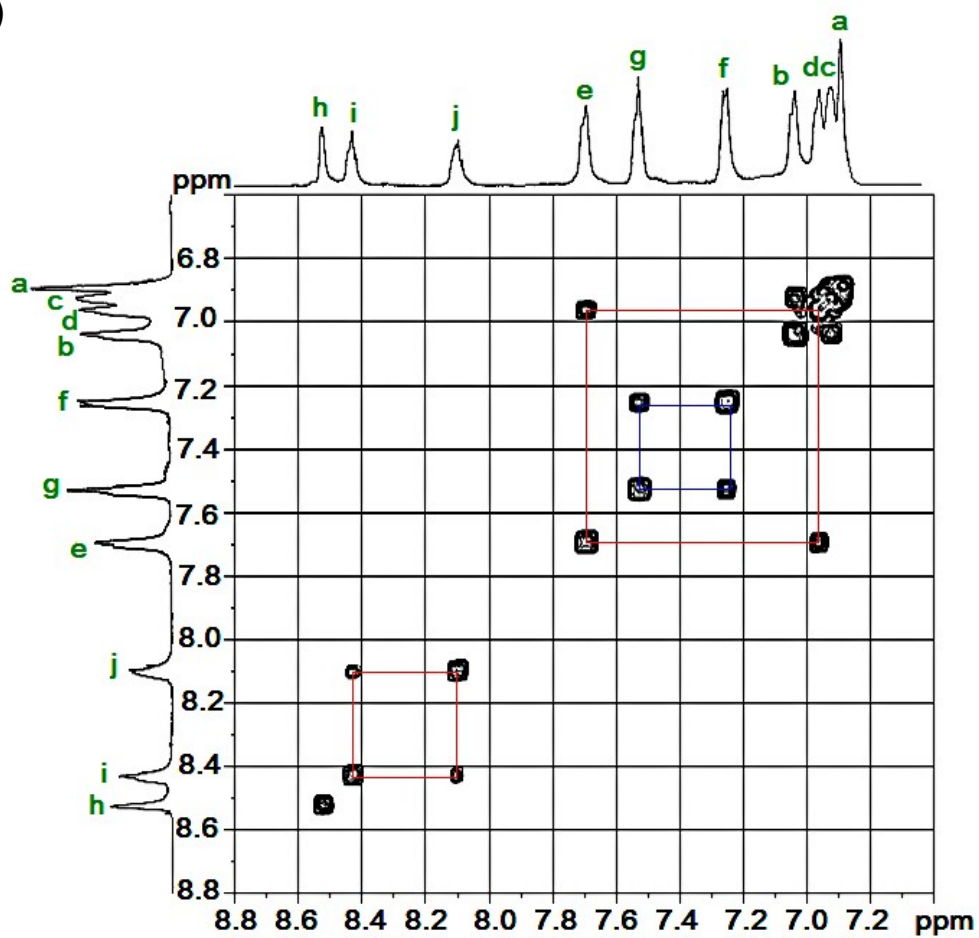


Fig. S7 (a) ¹H and (b) H-H COSY NMR spectra of PAI **6a** in DMSO-*d*₆.

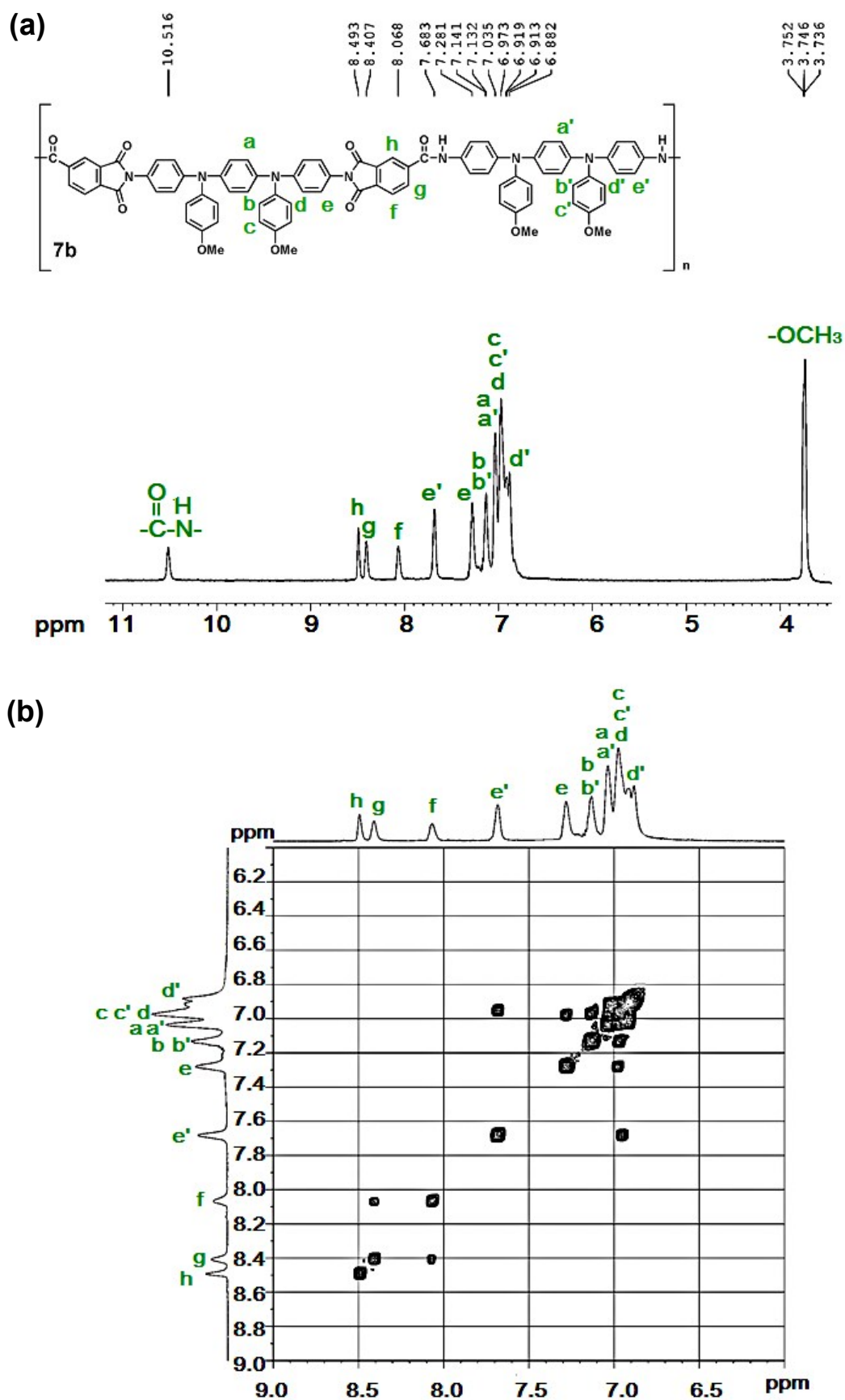


Fig. S8 (a) ^1H and (b) $\text{H}-\text{H}$ COSY NMR spectra of PAI **7b** in $\text{DMSO}-d_6$.

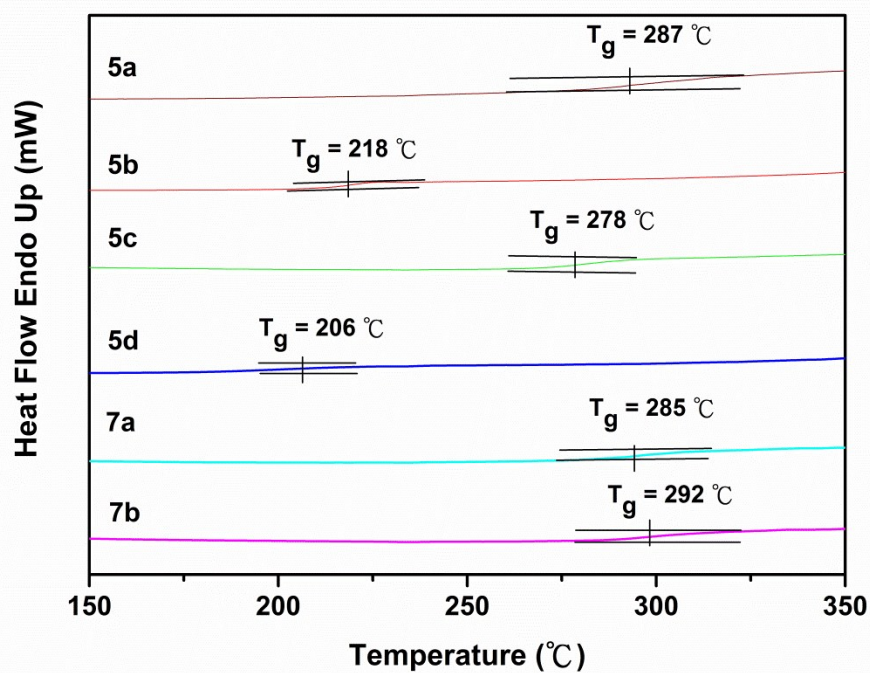


Fig. S9 DSC curves (the second scans after quenching from 400 °C) of all the PAIs with a heating rate of 20 °C min⁻¹.

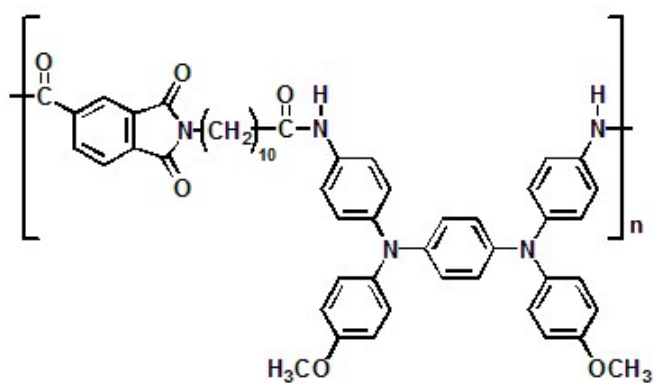
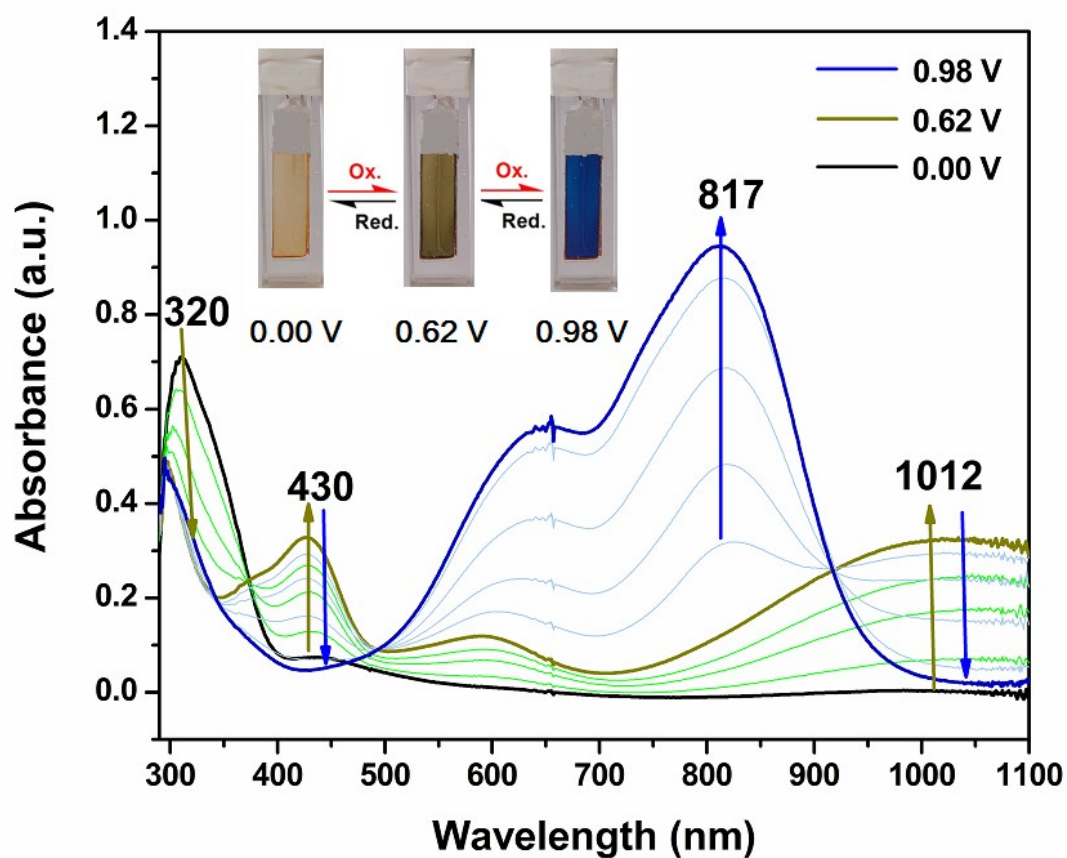


Fig. S10. Spectroelectrograms and color changes of **6d** thin film (190 ± 30 nm in thickness) on the ITO-coated glass substrate in 0.1 M $\text{Bu}_4\text{NClO}_4/\text{CH}_3\text{CN}$ at applied potentials of 0, 0.35, 0.45, 0.55, 0.65, 0.80, 0.85, 0.90, 0.95, and 0.98 V (vs Ag/AgCl) (Inset: polymer film with about $1.6 \mu\text{m}$ in thickness).

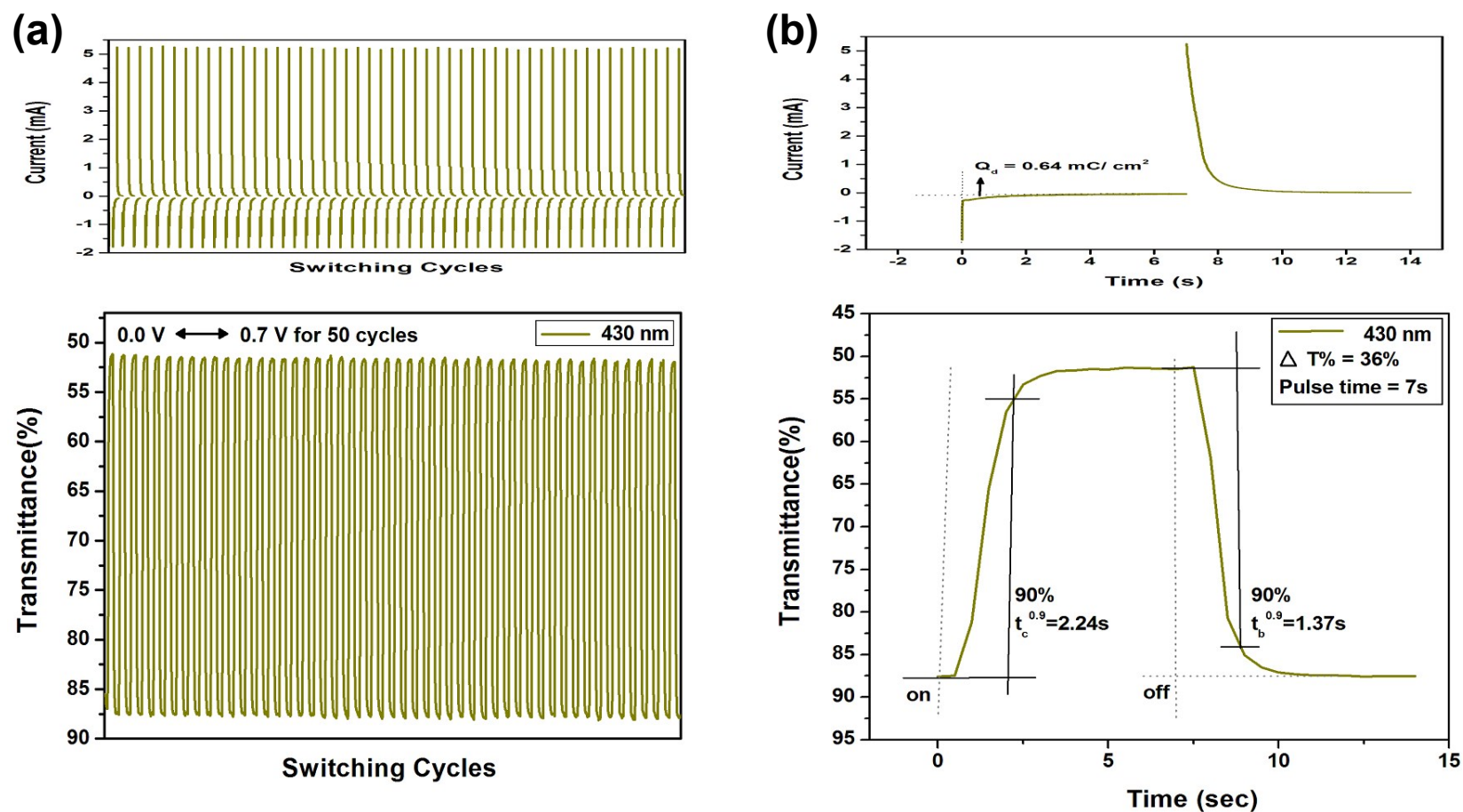


Fig. S11 Potential step absorptiometry of the cast films of **6d** on the ITO-glass slide (coated area ~ 1 cm²) (in CH₃CN with 0.1 M Bu₄NClO₄ as the supporting electrolyte) by applying a potential step: (a) optical switching at potential 0.00 V \leftrightarrow 0.70 V (50 cycles) and a switching time of 7 s, monitored at $\lambda_{\text{max}} = 430$ nm; (b) the 1st cycle transmittance change for the **6d** thin film.

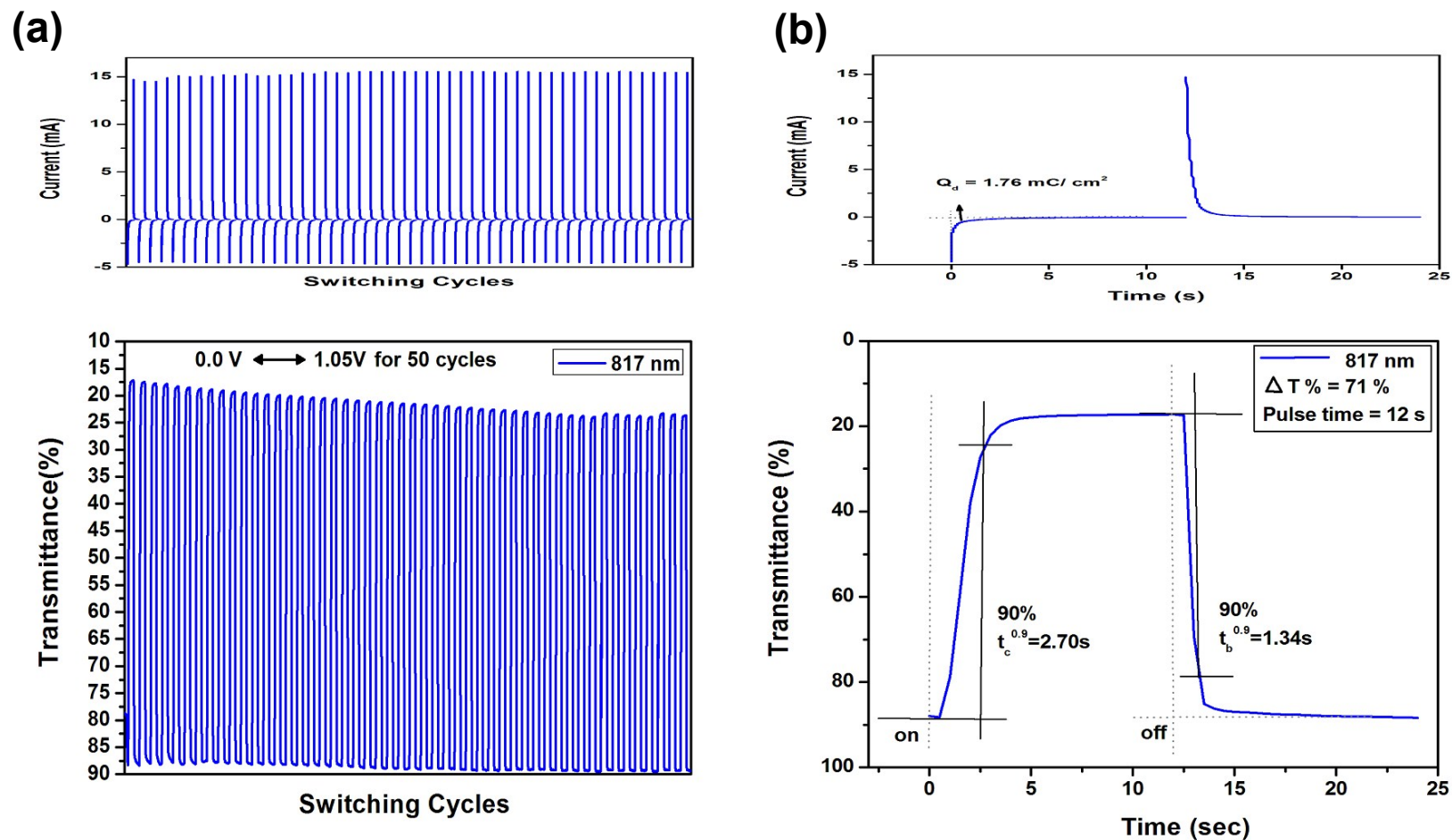
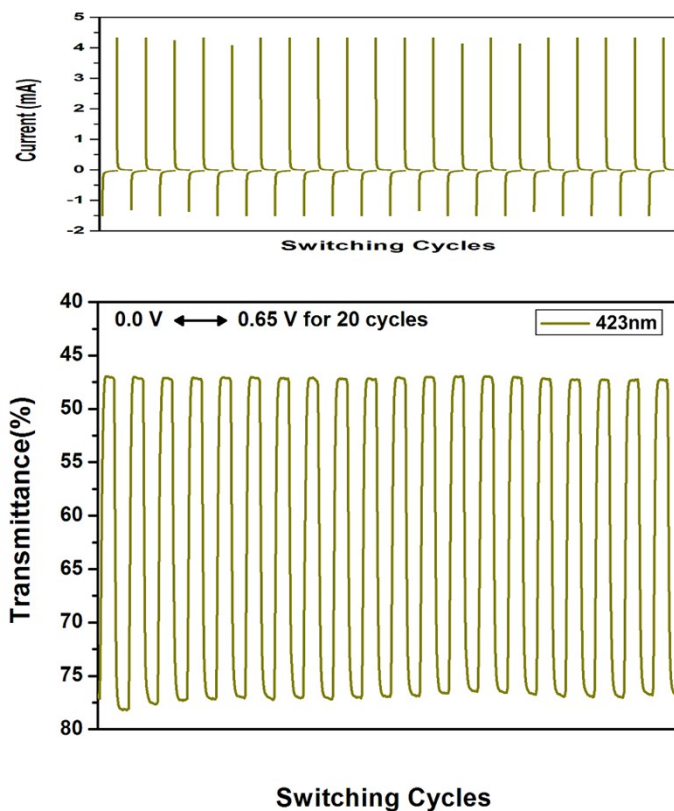


Fig. S12. Potential step absorptiometry of the cast films of **6d** on the ITO-glass slide (coated area $\sim 1 \text{ cm}^2$) (in CH_3CN with 0.1 M Bu_4NClO_4 as the supporting electrolyte) by applying a potential step: (a) optical switching at potential 0.00 V \leftrightarrow 1.05 V (50 cycles) and a switching time of 12 s, monitored at $\lambda_{\text{max}} = 817 \text{ nm}$; (b) the 1st cycle transmittance change for the **6d** thin film.

(a)



(b)

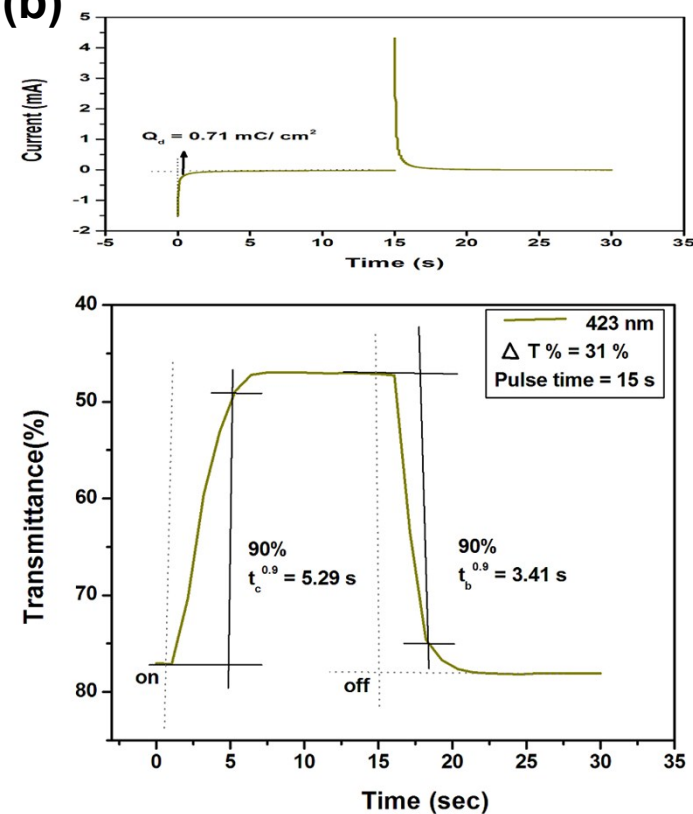


Fig. S13. Potential step absorptiometry of the cast film of **7b** on the ITO-glass slide (coated area $\sim 1 \text{ cm}^2$) (in CH_3CN with 0.1 M Bu_4NClO_4 as the supporting electrolyte) by applying a potential step: (a) optical switching at potential 0.00 V \leftrightarrow 0.65 V (20 cycles) and a switching time of 15 s, monitored at $\lambda_{\text{max}} = 423 \text{ nm}$; (b) the 1st cycle transmittance change for the **7b** thin film.

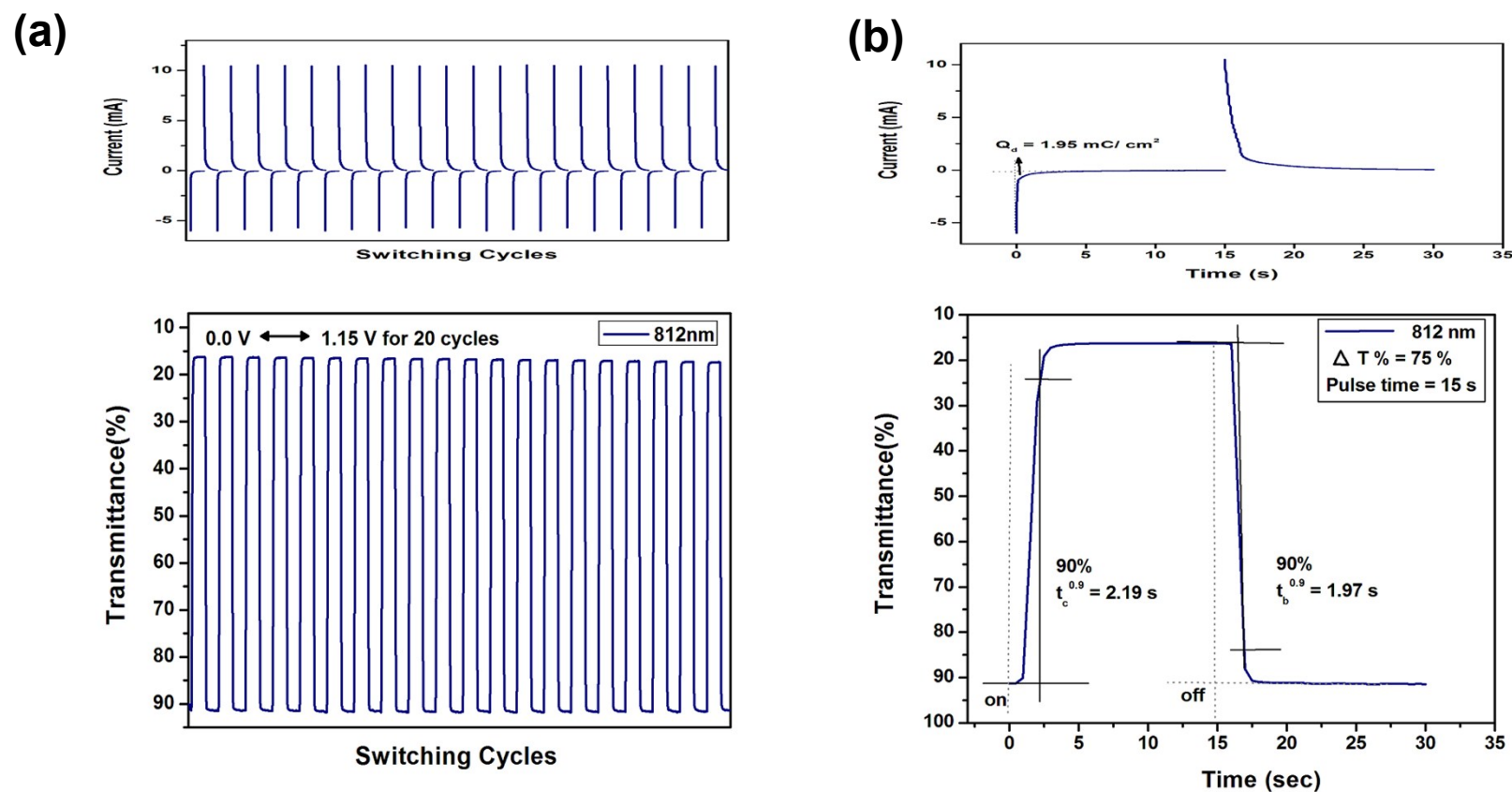


Fig. S14. Potential step absorptiometry of the cast film of **7b** on the ITO-glass slide (coated area $\sim 1 \text{ cm}^2$) (in CH_3CN with 0.1 M Bu_4NClO_4 as the supporting electrolyte) by applying a potential step: (a) optical switching at potential 0.00 V \leftrightarrow 1.15 V (20 cycles) and a switching time of 15 s, monitored at $\lambda_{\text{max}} = 812 \text{ nm}$; (b) the 1st cycle transmittance change for the **7b** thin film.